

**Mechanistic Investigation of Bacterial
3-Mercaptopyruvate Sulfurtransferase (3MST)
and Design of Inhibitors**

A thesis submitted to

Indian Institute of Science Education and Research – Pune

In partial fulfillment of the requirements for the BS-MS Dual Degree program

By

Saswata Nayak



Indian Institute of Science Education and Research, Pune

Dr. Homi Bhabha Road, Pashan, Pune-411008, India

April 2020

Supervisor: Dr. Amrita B. Hazra
Co-supervisor: Dr. Harinath Chakrapani

©Saswata Nayak 2020

All rights reserved


Dedicated to

*My parents, who sacrificed better prospects in life so I can pursue my
education,*

And my sister, for always being there.

CERTIFICATE

This is to certify that this dissertation entitled “**Mechanistic Investigation of Bacterial 3-Mercaptopyruvate Sulfurtransferase (3MST) and Design of Inhibitors**” towards the partial fulfilment of the B.S. – M.S. dual degree programme at the Indian Institute of Science Education and Research (IISER), Pune represents study/work carried out by Saswata Nayak at IISER Pune, under the supervision of Dr. Amrita B. Hazra (Assistant Professor, IISER Pune) and Dr. Harinath Chakrapani (Associate Professor, IISER Pune) during the academic year 2019-2020.



Saswata Nayak

IISER Pune

20151103



Dr. Amrita B. Hazra

IISER Pune

(Supervisor)



Dr. Harinath Chakrapani

IISER Pune

(Co-Supervisor)

Date: 6th April 2020

Place: Pune, Maharashtra, India

DECLARATION

I hereby declare that the matter embodied in the report entitled "**Mechanistic Investigation of Bacterial 3-Mercaptopyruvate Sulfurtransferase (3MST) and Design of Inhibitors**" are the results of the work carried out by me at the Department of Chemistry, IISER Pune, under the supervision of Dr. Amrita B. Hazra and Dr. Harinath Chakrapani and the same has not been submitted elsewhere for any other degree.



Saswata Nayak
IISER Pune
(20151103)



Dr. Amrita B. Hazra
IISER Pune
(Supervisor)



Dr. Harinath Chakrapani
IISER Pune
(Co-Supervisor)

Date: 6th April 2020

Place: Pune, Maharashtra, India

ACKNOWLEDGMENTS:

It gives me immense pleasure to acknowledge the people who have made this thesis possible.

I would like to thank my supervisor, *Dr. Amrita B. Hazra*, and my co-supervisor, *Dr. Harinath Chakrapani*, for their immense support and guidance throughout the tenure of this project. I have learnt a lot through working in their labs this past year. I also thank *Dr. Arnab Mukherjee* for agreeing to be on my thesis advisory committee.

I am immensely grateful to have such wonderful and supportive lab members, who would patiently take me through a journey of knowledge and mentor me. I will remain grateful to my mentors in the lab forever – *Yashwant bhaiya, Rupali, Mrutyunjay*, and *Suman*. I also thank *Yamini, Sheryl, Ateek* from Hazra lab and *Pooja, Prerona, Subhayan, Utsav, Anand, Farhan, Minhaj, Amal, Harshit, Gaurav*, and *Laxman* from Chakrapani lab for being amazing labmates and for creating a work-friendly environment in the lab.

I then turn to thank the instrument operators of NMR and Mr. Amit Bhat from the PerkinElmer facility at IISER Pune, who helped me get my data promptly. I thank IISER Pune for providing state-of-the-art facilities for scientific research and KVPY for the funding.

Above all, I am immensely thankful for having such wonderful friends whose constant support and motivation pulled me through my ups and downs during my life at IISER Pune. This page is too small to list all of them and thank them enough. And lastly, I would like to thank my parents and sister for being a constant pillar of support in all my ventures throughout my life. Without these people, this thesis would not have been possible.

CONTENTS:

❖ LIST OF FIGURES AND TABLES.....	7
❖ ABBREVIATIONS.....	8
❖ ABSTRACT.....	9
❖ INTRODUCTION.....	10
❖ MATERIALS AND METHODS.....	17
❖ RESULTS AND DISCUSSIONS.....	23
❖ CONCLUSIONS.....	41
❖ FUTURE DIRECTIONS.....	43
❖ REFERENCES.....	44

LIST OF FIGURES:

- **Figure 1:** Fenton reaction in the production of radical species
- **Figure 2:** Mechanism of turnover by 3MST
- **Figure 3:** Mechanism of turnover of the unnatural substrates by *Ec3MST*
- **Figure 4:** In-situ formation of 3-mercaptopyruvate ester
- **Figure 5:** Scheme for the deacetylation of unnatural substrates
- **Figure 6:** SDS-PAGE gel for protein purification
- **Figure 7:** Methylene blue assay for unnatural substrates with wild-type, R179L, R188L, and R179L/R188L *Ec3MST*
- **Figure 8:** Intrinsic fluorescence assay of the unnatural substrates with wild-type, R179L, R188L, and R179L/R188L *Ec3MST*
- **Figure 9:** F/F_0 plots for comparison of decrease in fluorescence intensity
- **Figure 10:** Sequence alignment of h3MST and *Ec3MST*
- **Figure 11:** Molecular modeling of *Ec3MST* wild-type based on the structure of h3MST
- **Figure 12:** The docked structure of 3-mercaptopyruvate in the active-site of *Ec3MST* wild-type
- **Figure 13:** The docked structure of compound **3** in the active-site of wild-type *Ec3MST*
- **Figure 14:** The docked structure of de-acetylated compound **1b** in the active-site of wild-type *Ec3MST*
- **Figure 15:** Methylene blue assay of unnatural substrates with human 3MST and *Ec3MST*
- **Figure 16:** Active-site residue comparison of h3MST and *Ec3MST*

LIST of TABLES:

- **Table 1:** List of compounds used in this study
- **Table 2:** Rates for the reaction of the substrates with the enzymes wild-type, R179L, R188L, and R179L/R188L *Ec3MST*, along with the absorbance recorded at t=15 minutes in the Methylene Blue assay

ABBREVIATIONS:

NMR	Nuclear Magnetic Resonance
DMSO	Dimethyl sulfoxide
mg	milligram
mL	millilitre
mmol	millimole
M	molar
3MST	3-Mercaptopyruvate sulfurtransferase
<i>Ec</i> 3MST	<i>Escherichia coli</i> 3MST
h3MST	human 3MST
CBS	Cystathionine beta synthase
CSE	Cystathionine gamma lyase
DTT	Dithiothreitol

ABSTRACT:

Hydrogen sulfide (H₂S) gas has been found to have a cytoprotective role in bacteria and is also linked with many important physiological functions in humans. We are exploring the mechanism of H₂S production by 3-mercaptopyruvate sulfurtransferase (3MST) from *Escherichia coli* using unnatural substrates comparing it with the mechanism reported for 3-mercaptopyruvate, the natural substrate of the enzyme. Our lab has previously developed these molecules that can produce varying amounts of H₂S in the *in-vitro* reaction with wild-type *E. coli* 3MST. The structure of these substrates differs vastly from 3-mercaptopyruvate – a non-polar aromatic group has been substituted in place of the highly polar carboxyl group of 3-mercaptopyruvate. Arginine residues in the active-site (Arg 179 and Arg 188) of the enzyme have been reported to hold the substrate in the active-site by electrostatic interactions with the carboxyl and carbonyl groups of 3-mercaptopyruvate. In this study, we investigate the mechanistic details of the turnover of these unnatural substrates by the *Ec*3MST enzyme by the site-directed mutagenesis of these arginine residues and quantifying the amount of H₂S produced in the enzymatic reaction by the Methylene Blue assay. We also computationally dock the unnatural substrates in the active-site of the wild-type *Ec*3MST enzyme to visualize the interactions with the active-site residues. Lastly, we clone and purify the human 3MST enzyme and characterize it using the unnatural substrates.

In conclusion, we establish that a new π -cation interaction is responsible for stabilizing the aromatic group of the unnatural substrates in the active-site, compensating for the loss of the electrostatic interaction with the carboxyl group of 3-mercaptopyruvate. Moreover, the mutation of the Arg 179 to a leucine residue increases the activity of the enzyme significantly, which is not observed in the R188L *Ec*3MST mutation. We also conclude that although human 3MST enzyme has similar active-site residues as the *Ec*3MST, the amount of H₂S produced in the reaction of human 3MST and the unnatural substrates is significantly less as compared to *Ec*3MST.

1. INTRODUCTION:

Hydrogen sulfide has been synonymously associated with toxicity and its distinctive rotten egg odor. It has been historically regarded as a respiratory and metabolic poison⁽¹⁾, until the pathway facilitating the production of H₂S by the interconversion of cysteine, homocysteine was discovered from liver homogenates^(2,3). Further detailed biochemical characterization of cystathionine beta synthase (CBS), cystathionine gamma lyase (CSE), and 3-mercaptopyruvate sulfurtransferase (3MST) established the biogenesis of H₂S pathways. H₂S has a significant role in cellular physiology, as shown by multiple studies. It was detected in healthy human and animal brain tissues^(4,5), it was found to help relax vascular smooth muscles⁽⁶⁾, and it regulates angiogenesis, energy metabolism, apoptosis, and inflammation^(7,8). It has also been associated with cytoprotectivity and can directly scavenge free radical species⁽⁹⁾. Due to its myriad role in physiology, it has been regarded as a gasotransmitter⁽¹⁰⁾, a gaseous signaling molecule.

One of the fascinating roles of H₂S that has been shown in a study⁽¹¹⁾ is its ability to help bacteria survive against the onslaught of antibiotics. When challenged with different classes of antibiotics, the strain of *E. coli* lacking the H₂S producing enzyme (3MST) survives worse as compared to the wild-type strain. But, when NaHS (an inorganic salt) was added before the challenge, the strain's survival was comparable to the wild-type. This trend was again observed in three other evolutionary distant bacterial pathogenic species – *Bacillus anthracis*, *Staphylococcus aureus*, and *Pseudomonas aeruginosa*. When their respective H₂S producing enzymes were knocked out (3MST, in case of *E. coli*), or when the bacterial cells were pre-incubated with known inhibitors of CBS/CSE (for *S. aureus* and *P. aeruginosa*), they survived worse than the native strains. But the addition of NaHS prior to the antibiotic challenge improved their survival. The authors further show that H₂S plays an important role in sequestering free iron, which would otherwise participate in the genotoxic Fenton reaction (**Figure 1**).

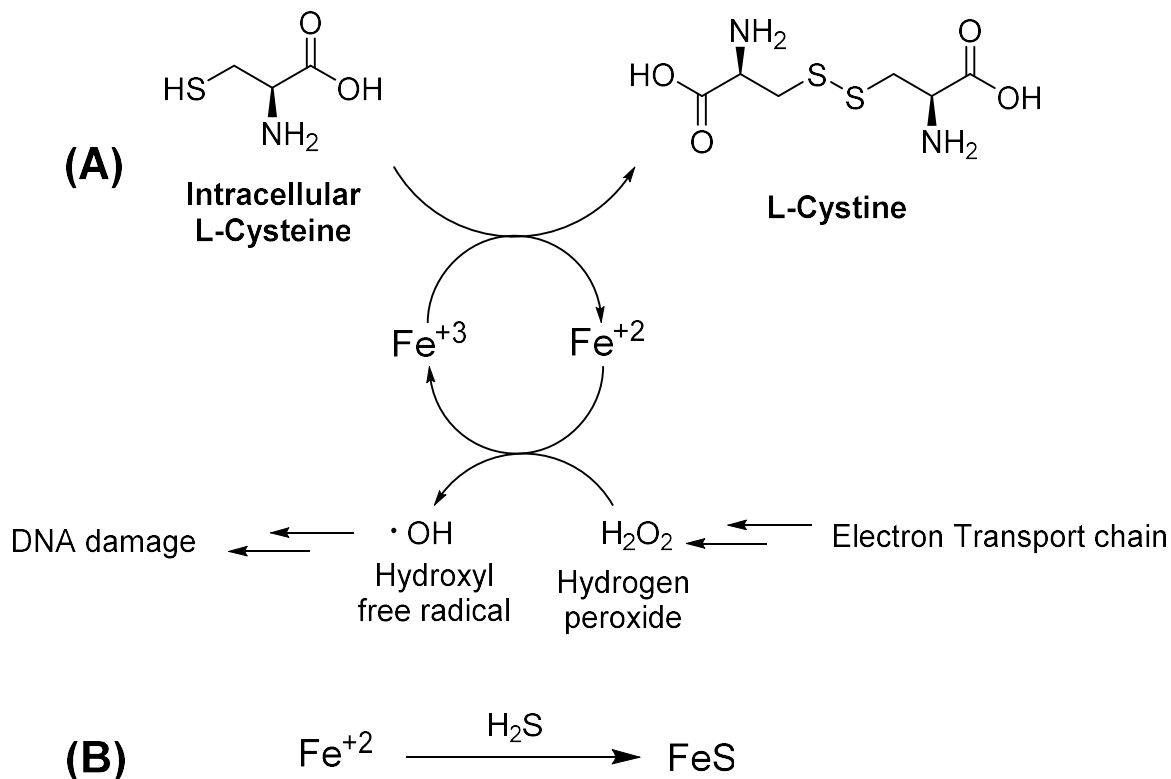


Figure 1: (A) The Fenton reaction is promoted by high levels of intracellular L-Cysteine, where L-Cysteine is converted to L-Cystine by the reduction of Fe^{+3} to Fe^{+2} . This Fe^{+2} , in turn, can generate hydroxyl free radicals from H_2O_2 by the Fenton reaction, and it is known to cause DNA damage. (B) H_2S can sequester the Fe^{+2} required for the genotoxic Fenton reaction by converting it into non-toxic FeS.

These findings were in direct agreement with a previous study⁽¹²⁾, which showed that various classes of bactericidal antibiotics ultimately generate reactive oxygen species, which is responsible for cell death.

Multiple studies show how H_2S contributes to the reduction of ROS in a cell. One study⁽¹³⁾ shows that under antibiotic stress conditions, H_2S targets the copper-heme containing cytochrome bo oxidase (CyoA), thus inhibiting the more-efficient respiration pathway. This forces the cell to fall back on the less energy-efficient cytochrome bd oxidase (CydB) for respiration. Hence, the amount of $\text{O}_2^{\cdot-}$ radical produced from the electron flux (from the electron transport chain) is further reduced due to slower respiration. So, this is also

a way in which H₂S can reduce the number of free radicals. Apart from these, H₂S has been shown to directly scavenge free radical species like ROS, peroxynitrite, and hypochlorite^(14,15). Although the role of H₂S in relieving oxidative stress from bacteria has been undeniable, the correlation of antibiotic stress with increased ROS levels has not been convincingly proved.

A study⁽¹⁶⁾ challenges this proposition by demonstrating that the cell viability does not change significantly when incubated with bactericidal antibiotics in oxygen-rich or oxygen-deficient media. The levels of H₂O₂ in the culture medium of *E. coli* did not change significantly when challenged with an antibiotic. Moreover, when the ROS scavenging enzymes catalase and peroxidase were knocked out from the *E. coli* strain, there was no significant difference in cell viability as compared to the wild-type during an antibiotic challenge. Thus, there exists a debate on whether the downstream consequence of all antibiotic challenges results in the increase of ROS in the cells.

Moving on to the mechanism of turnover of 3-mercaptopyruvate by 3MST, this mechanism has been investigated by multiple studies⁽¹⁷⁻¹⁹⁾. The catalytic loop in the active-site – CGSGVT, is conserved across all 3MSTs, which has been reported⁽¹⁸⁾ to be responsible for the deprotonation of the active-site cysteine residue, which can then act as a nucleophile. This de-protonated Cys residue can perform a nucleophilic attack on the thiol group of 3-mercaptopyruvate, thus getting persulfurated (**Figure 2 (A)**). The sulfur on 3MST can then be taken up by a sulfur acceptor, like glutathione, thioredoxin, dithiothreitol, or even a Cys residue of a protein⁽²⁰⁾. Another nucleophile can further attack this sulfur, to release H₂S (**Figure 2 (B)**), or the sulfur can be further propagated into a signaling pathway (**Figure 2 (C)**) which is dependent on the persulfuration of a signaling protein in the pathway. It can also be converted into polysulfides, which too can act as a signaling molecule or as a sulfur source for other physiological processes (**Figure 2 (D)**).

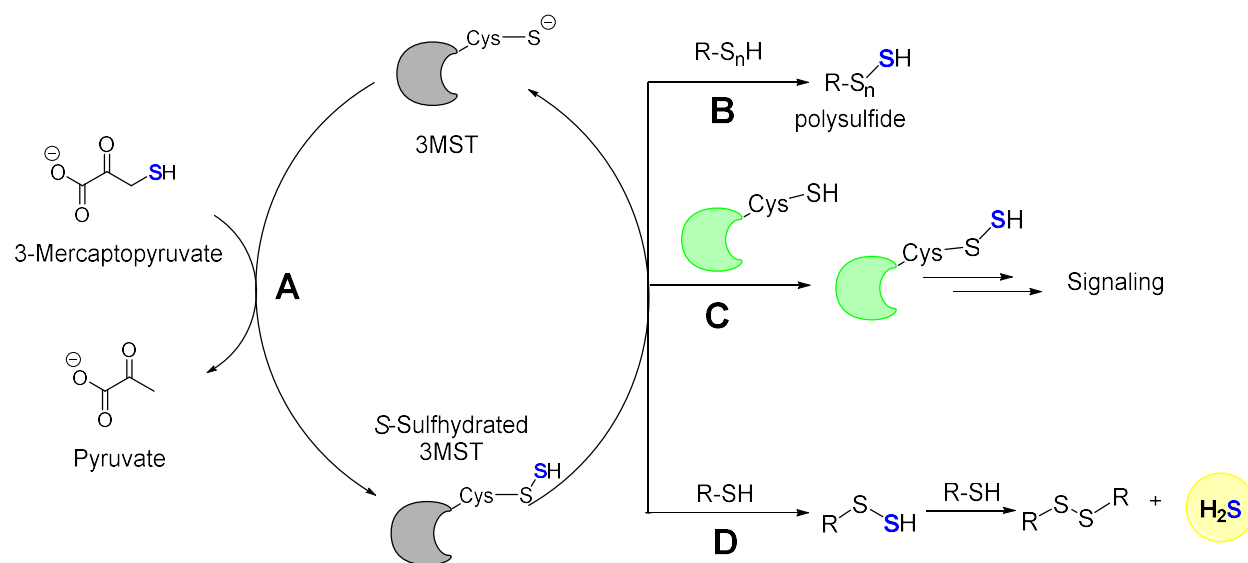


Figure 2: Mechanism of turnover of 3-mercaptopyruvate by 3MST, and the fate of the sulfur of 3-mercaptopyruvate in the physiology.

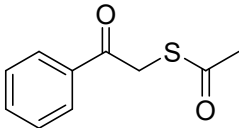
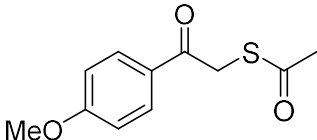
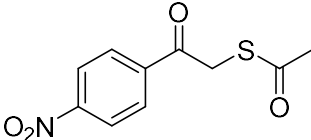
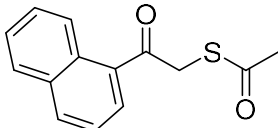
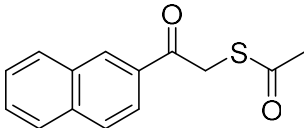
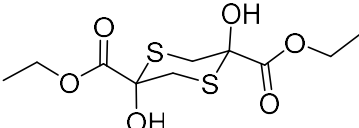
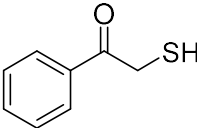
In our lab during the early stages of the project, we wanted to investigate whether H₂S can be produced in target cells in desirable concentrations by the already-present machinery – the H₂S producing enzymes. We had decided to work with *E. coli* as our model system since the major H₂S producer in *E. coli* is 3MST, and the other well-known H₂S producing enzymes – CBS/CSE were absent in *E. coli*. It adds to our advantage that *E. coli* is an extensively studied system, and genetic modifications are relatively simple. Also, the crystal structure of *Ec*3MST is available (PDB: 1URH), which opens up avenues for computational studies like molecular docking.

In unpublished data from our lab, we have synthesized compounds (**Table 1**) that can act as unnatural substrates for *E. coli* 3MST and it has been observed that they can produce varying amounts of H₂S enzymatically. The mechanism of formation of H₂S from the compounds is shown in **Figure 3**.

The thiol groups of the compounds **1a-e** are de-acetylated in the presence of dithiothreitol (DTT), which is used in the assay used in this study for the quantification of H₂S produced in the enzymatic reaction. If we compare the structure of the compounds in **Table 1 (1a-e**, with the thiol de-protected) with the structure of the natural substrate 3-

mercaptopyruvate (**Figure 4 (B)**), we can see that in the unnatural substrates, the carboxyl group has been replaced with a non-polar aromatic group. Due to the change from a highly polar group to a highly non-polar group in the structure of the substrate, it is fascinating that the enzyme can still turn over the unnatural substrates.

Table 1: Compounds used in this study* :

Entry	Structure	Compound code
1		1a
2		1b
3		1c
4		1d
5		1e
6		2
7		3

* Synthesis of compounds in Table 1 are designed and synthesized by Mrutyunjay Mair and Suman Manna, IISER Pune

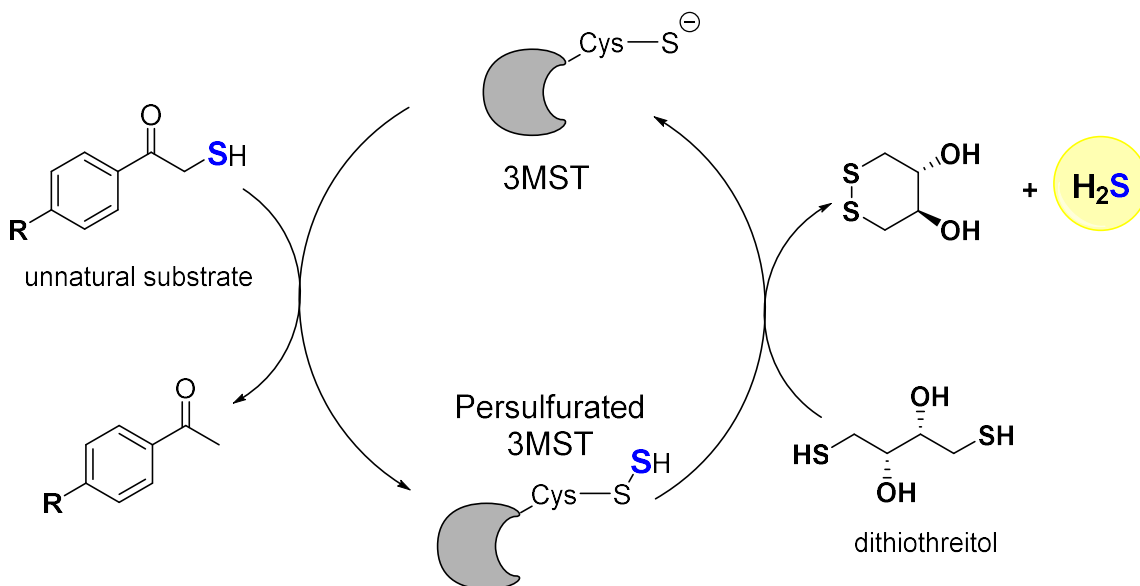


Figure 3: The mechanism of turnover of the unnatural substrate by wild-type *Ec3MST* enzyme.

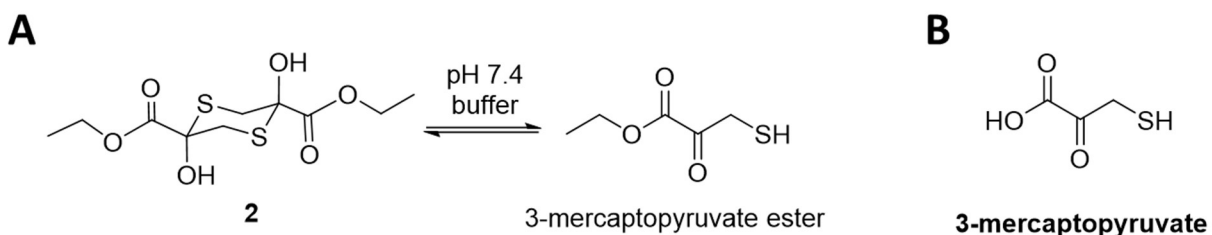


Figure 4: (A) The ethyl ester of 3-mercaptopyruvate is generated *in-situ* by the dissociation of the compound **2** in the HEPES-NaOH pH 7.4 buffer. (B) The structure of 3-mercaptopyruvate

In this study, we are using the compound **2** due to the unavailability of 3-mercaptopyruvate commercially. 3-mercaptopyruvate and its ethyl ester show similar reactivity with the wild-type, R188L, R179L, and R179L/R188L *Ec3MST* enzymes, and hence has been used in place of the natural substrate 3-mercaptopyruvate.

Two crystal structures of the human 3MST (h3MST) have been reported – one with pyruvate as a ligand (PDB ID: 4JGT) and another without a ligand (PDB ID: 3OLH) bound

in its active-site. It was shown in that study⁽¹⁷⁾ that in h3MST, two arginine residues (Arg 188 and Arg 197) were primarily responsible for electrostatically binding the 3-mercaptopyruvate molecule in the active-site. The cysteine present in the active-site (Cys 247) acts as a nucleophile and attacks on the thiol group of the 3-mercaptopyruvate, releasing pyruvate. A sulfur acceptor would then desulfurate the persulfurated cysteine residue, and in turn, would undergo oxidation to release H₂S gas.

Another study⁽¹⁸⁾ created point mutations of the two arginine residues to leucine in *Ec3MST* and reported a 700 – 2000-fold decrease in k_{cat} of the overall reaction for R179L, R188L, and R179L/R188L mutants. The study also suggests that the absence of one arginine is compensated by the other arginine residue, and hence can still catalyze the reaction.

In this study, we have focused on the molecular basis for the turnover of the unnatural substrates developed in our lab. The specific aims of the project are:

- Modeling of *Ec3MST* protein and docking of unnatural substrates in its active-site to visualize the interactions of the residues and substrates
- Probing the role of arginine residues of the active-site in turnover of the unnatural substrates by site-directed mutagenesis

2. MATERIALS AND METHODS:

2.1. Experimental section:

Compound **3** was synthesized by the de-protection of the acetate group of the compound **1a**, following the scheme showed in **Figure 5**.

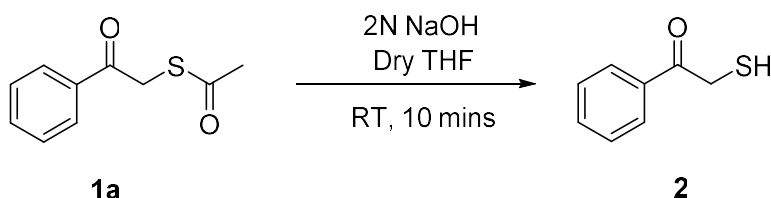


Figure 5: Synthesis of compound **2**

Synthesis of compound **2**:

The compounds were taken in a two necked round bottom flask and dissolved in dry tetrahydrofuran (9 mL THF per millimole of **1a**) under nitrogen atmosphere. The reaction mixture was stirred at room temperature, followed by dropwise addition of NaOH. The reaction was quenched by the addition of excess 2N HCl at 10 minutes. This was transferred into a separating funnel, and dichloromethane (DCM) was added into it – which led to a clear separation of the organic layer and the aqueous layer. The aqueous layer was washed with 2 x 10 mL of DCM, and the organic layer was collected. The organic layer was washed with saturated brine solution to get rid of the excess HCl, and then it was dried over anhydrous Na₂SO₄, and concentrated under reduced pressure.

Overexpression and purification of wild-type, R179L, R188L, R179L/R188L Ec3MST, and h3MST:

Protein overexpression: The genes of wild-type, R179L, R188L, and R179L/R188L Ec3MST, was cloned from the genome of wild-type *E. coli* K-12 MG1655 into pET28a vector using restriction-free cloning strategy. The gene of h3MST was also cloned into

the pET28a vector[†]. These plasmids were transformed into *E. coli* DH5- α strain for cloning, followed by extraction of the plasmids and a second transformation of the plasmid to *E. coli* BL21 (DE3) cells for overexpression of the respective proteins.

The BL21 (DE3) strains of the respective proteins were grown overnight in Luria-Bertani (LB) broth with kanamycin (25 μ g/mL) at 37°C with constant shaking at 180 rpm. These cultures were then transferred to large secondary cultures (1 liter) of LB broth with kanamycin (25 μ g/mL) with 0.5% of inoculum. They were incubated at 37°C with constant shaking at 180 rpm, till the O.D.₆₀₀ reached 0.6. To these cultures, Isopropyl β -D-1-thiogalactopyranoside (IPTG) was added to a concentration of 1mM to induce the protein overexpression, followed by incubation of the cultures at 18°C with constant shaking at 180 rpm, for 14 hours.

The cells were harvested post-induction by centrifuging the culture at 6500 rpm at 4°C for 10 minutes. The cell pellets obtained were flash-frozen in liquid nitrogen and then stored in -80°C, till further use.

Protein purification: The protein purification was done by using Ni-NTA affinity chromatography. The cell pellets were resuspended in cold lysis buffer consisting of 50 mM Tris-HCl pH 8.0, 300 mM NaCl, 10 mM MgCl₂, 30 μ M Phenylmethylsulfonyl fluoride (PMSF), and 0.03% β -mercaptoethanol (BME) by sonication on ice for 15 minutes (1 second “on” and 3 seconds “off” at 60% amplitude). The cell debris was separated from the supernatant containing the proteins by centrifuging the sonicated cells at 18000 rpm at 4°C for 30 minutes. If the supernatant appeared cloudy, with some suspended matter in it, it was passed through a 0.22 μ m syringe filter and loaded on to a Ni-NTA column, which was already equilibrated with the lysis buffer used for the lysis of the cell pellet. As the supernatant was loaded, a small amount of the flow-through was collected for checking the loss of protein – which would indicate the poor binding of the protein with the column. The column was then washed with around 5 column volumes of two wash

[†] Cloning of wild-type, R188, R179L, R179L/R188L Ec3MST and h3MST was done by Rupali Sathe, Mrutyunjay Nair and Yamini Mathur, IISER Pune

buffers having 5 mM and 25 mM Imidazole, 50 mM Tris-HCl pH 8.0, 300 mM NaCl and 0.03% of β -mercaptoethanol (BME), while simultaneously collecting the eluted fractions and immediately storing them on ice. Following the column wash by the wash buffers, the bound proteins are eluted with the elution buffer, comprising 250 mM Imidazole, 50 mM Tris-HCl pH 8.0, 300 mM NaCl and 0.03% of β -mercaptoethanol (BME), simultaneously collecting the eluted protein in 1 mL fractions and again, storing them on ice. Using the Bradford assay, it was determined whether the protein has stopped eluting; and the fractions containing the pure protein were determined by running an SDS-PAGE gel. The pure protein fractions were pooled and were buffer-exchanged in a desalting buffer containing 50 mM Tris-HCl pH 8.0, 100 mM NaCl and 0.03% β -mercaptoethanol (BME) using Econo-Pac 10 DG pre-packed desalting columns (BioRad). A 10% v/v glycerol solution of the protein was made and was flash-frozen in liquid nitrogen, and stored in -80°C until further use. The concentration of the protein was determined by measuring the absorbance of the solution at 280 nm in a UV-vis spectrophotometer. The value of the molar extinction coefficient was obtained from ProtParam from its amino acid sequence.

Methylene blue assay for the detection of enzymatic H₂S production:

Methylene blue is a colorimetric assay, commonly used to detect H₂S⁽²¹⁾. The reaction mixture consists of the enzyme, the compound of interest, zinc acetate and dithiothreitol (DTT) in a HEPES buffer, pH 7.4. DTT is added as it would act as a nucleophile and would release H₂S from the persulfurated cysteine in the active-site of 3-mercaptopyruvate sulfurtransferase (3MST). The H₂S gas evolved from the reaction would be trapped in the reaction mixture as Zinc sulfide (ZnS) by the reaction of H₂S with zinc acetate.

For the assay, a 2 mL reaction mixture contained 200 mM HEPES-NaOH buffer (pH 7.4), 400 μ M of Zn(OAc)₂·2H₂O (from 40 mM stock prepared in deionized water), 1 μ M of the respective enzyme and 10 mM of DTT (added from a 100 mM stock prepared in deionized water). Based on the desired concentration, the compound was added from its DMSO stock, followed by adjusting the total DMSO in the reaction mixture to 2%.

The reaction time is calculated from the time of addition of the compound in the reaction mixture. The reaction mixtures were incubated at 37°C without shaking.

Simultaneously, in 0.6 mL tubes, a mixture of 200 μ L of FeCl₃ (30 mM stock in 1.2 M HCl) and 200 μ L of *N,N*-Dimethyl-*p*-phenylenediamine sulfate (DMPPDA) (20 mM stock in 7.2 M HCl) were mixed. To this tube, at the chosen time points, 200 μ L aliquots of the reaction mixture were added. Then these tubes were incubated at 37°C for 30 minutes to allow for the Methylene blue dye to form. Post incubation, aliquots of 150 μ L was added in each well on a transparent 96-well plate, and the absorbance values were measured at 676 nm using a microplate reader (Thermo Scientific VarioskanFlash).

Intrinsic fluorescence spectra of the enzymes when co-incubated with various compounds:

In this experiment, stocks of all the enzymes were made in 200 mM HEPES-NaOH pH 7.4 buffer such that the final concentration of the enzyme in them was 20 μ M. The stock solutions of each of the compounds were freshly made in DMSO and then diluted to the desired concentration (150 μ M for compound **2**, 300 μ M for compound **3**) using 200 mM of HEPES-NaOH buffer pH 7.4. The final concentration of DMSO in each of the compound stocks was adjusted to 4% (v/v). Then, in an opaque black 96-well plate, 75 μ L of the enzyme stock and 75 μ L of the compound stock were added carefully in a well using a pipette, followed by gentle mixing in order to avoid any air bubbles. This procedure was done in triplicates in three separate wells in order to have three separate instances for the enzyme and the compounds to interact. Thus, in each well the final concentration of the enzyme was 10 μ M and 75 μ M of compound **2** or 150 μ M of compound **3** were present.

The emission spectra of the enzyme and compound mixture was recorded in a microplate reader (PerkinElmer EnSight), from 305 nm to 450 nm at an interval of $\lambda=5$ nm with $\lambda_{\text{excitation}}=287$ nm.

2.2. Computational section

Molecular docking:

AutoDock 4.2⁽²²⁾ is a commonly used stand-alone software used for computationally docking small molecules in protein structures. This was used for docking our ligand of interest in the active-site of *Ec*3MST. The structures of the ligands were drawn in ChemDraw Professional, and the structure geometry was optimized in it. These were then exported as .pdb files, which is readable by the AutoDock software. In the software, all the heteroatoms (like water) and external ligands were removed from the protein file, followed by adjusting the charge on the proteins. Only the polar hydrogens were added on to the protein, and the protonation on the Histidine residues near the active-site was manually adjusted. A fine calculation grid (size = 0.1 Å) was created on the active-site, encapsulating all the residues approximately within a 5 Å radius from the presumed binding site of 3MST. The same grid dimensions were used for all the docking experiments conducted using that particular enzyme. Both the ligand and the protein were converted from .pdb format to a much simpler .pdbqt format, which is recognizable by the AutoDock software.

Since two arginine residues are present in the active-site, they were made flexible, while the rest of the protein molecule was to be considered rigid by the software. Once we have both the ligand and protein .pdbqt files, and the grid dimensions file, we can run the process. The Genetic Algorithm was utilized for the docking calculations, which would generate 50 models of the ligand in different conformations. From these conformations, the model which had the proper orientation of the sulfur with respect to the cysteine sulfur was taken into consideration. Among them, the conformation having the highest binding energy was taken, since it would be very close to what the ligand would look like in the active-site of the enzyme. The protein-ligand structure was then minimized in the Chimera software to remove any clashes or contacts present in the complex.

Modeling *Ec3MST* protein structure from h3MST structure (PDB ID: 4JGT):

Modeling of *Ec3MST* was done with the reported structure of the h3MST (PDB ID: 4JGT) as the template on an online server for protein structure and function prediction, named I-TASSER^(23, 24). I-TASSER was chosen to model the *Ec3MST* due to its easily interpretable graphical user interface. Since the reported crystal structure of *Ec3MST* (PDB ID: 1URH) did not have any ligands bound to it, the active-site residues were not in the correct conformation for doing docking experiments. Human 3MST has a high sequence identity (% identity = 40.5%) and very high secondary structure similarity (TM-score = 0.8930) when compared with the reported crystal structure of *Ec3MST* (PDB ID:1URH). Moreover, the active-site residues are conserved across both the proteins. Hence, it was an ideal template for modeling *Ec3MST*.

A .pdb file of h3MST was given as the template (with only one chain and after removing all the heteroatoms), and the sequence of *Ec3MST* was entered in FASTA format. The program was constrained to output models having the exact secondary structures as found in the crystal structure of *Ec3MST* (PDB ID: 1URH). The output file was used for the docking experiments with *Ec3MST*.

3. RESULTS AND DISCUSSIONS

Overexpression and Purification of proteins:

The wild-type, R179L, R188L, R179L/R188L *Ec3MST*, and h3MST enzymes were cloned in the pET28a vector system. The proteins were purified using Ni-NTA affinity chromatography and their purity was checked on an SDS-PAGE gel (**Figure 6**).

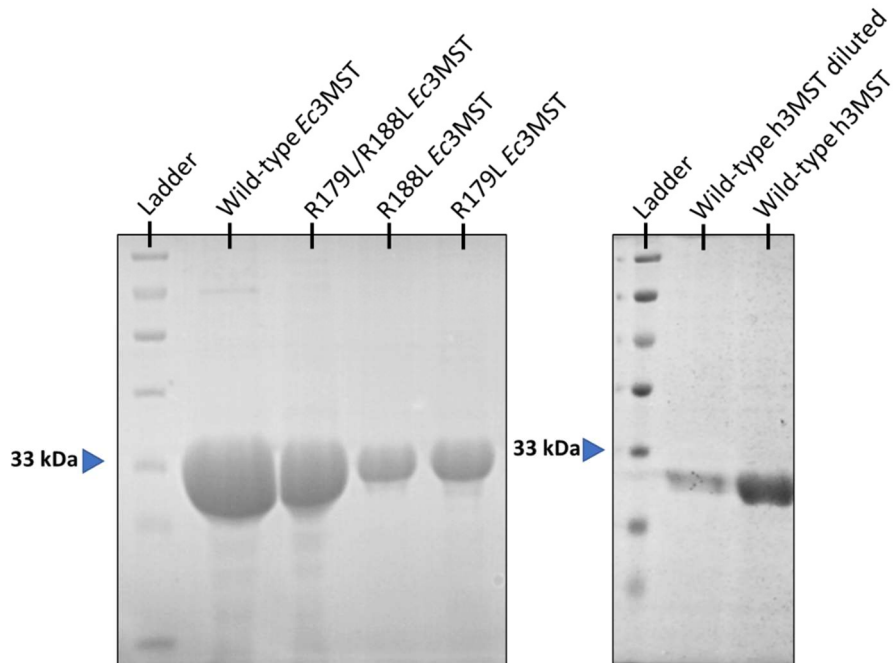
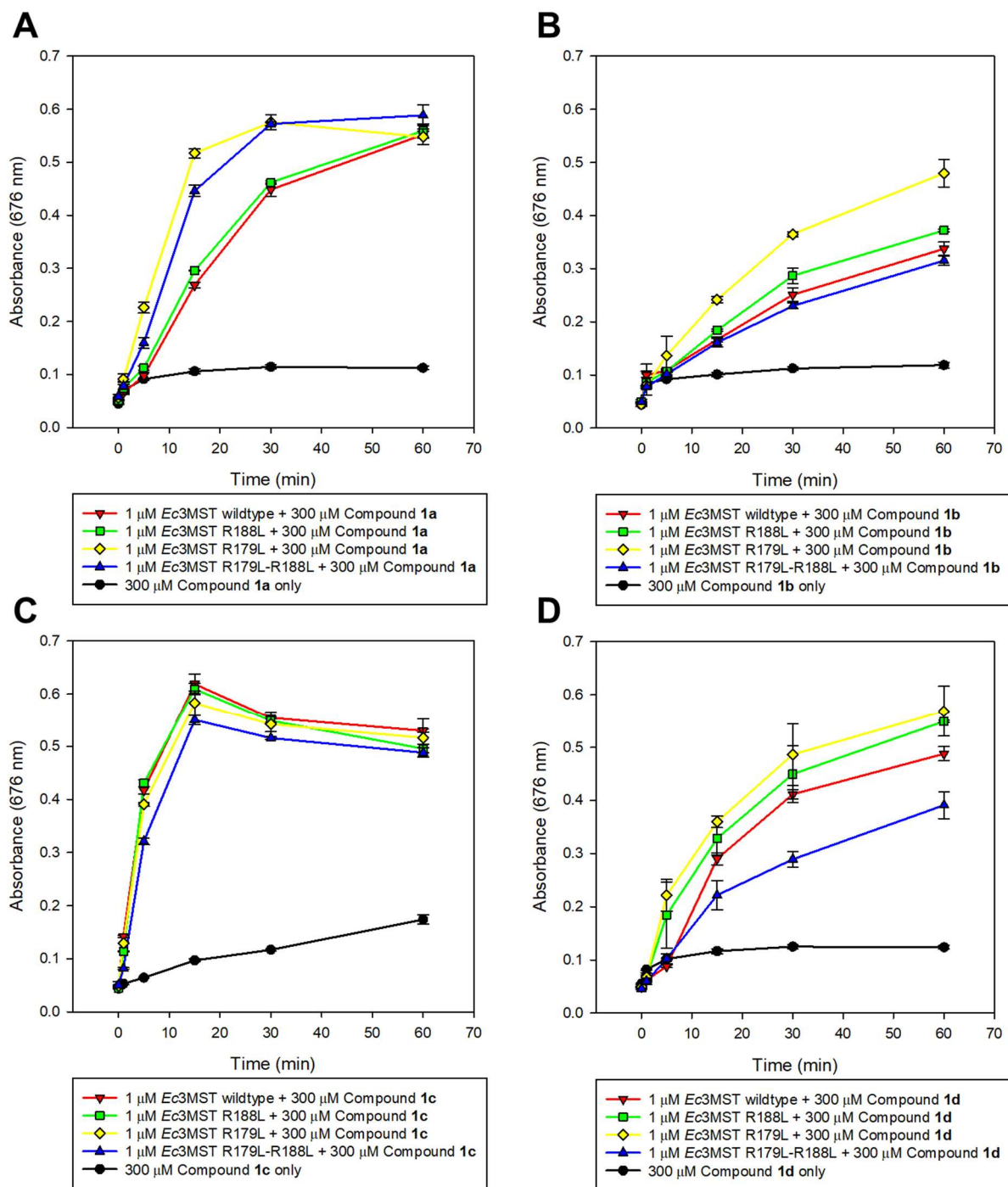


Figure 6: SDS-PAGE gel image showing all the purified proteins. The molecular weight of the proteins \approx 33kDa.

Monitoring the production of H₂S using the Methylene Blue assay:

The production of H₂S by the reaction of wild-type, R179L, R188L, and R179L/R188L *Ec3MST* and the substrates was monitored using the Methylene Blue assay. The plots for the absorbance versus time are shown below (Figure 7).



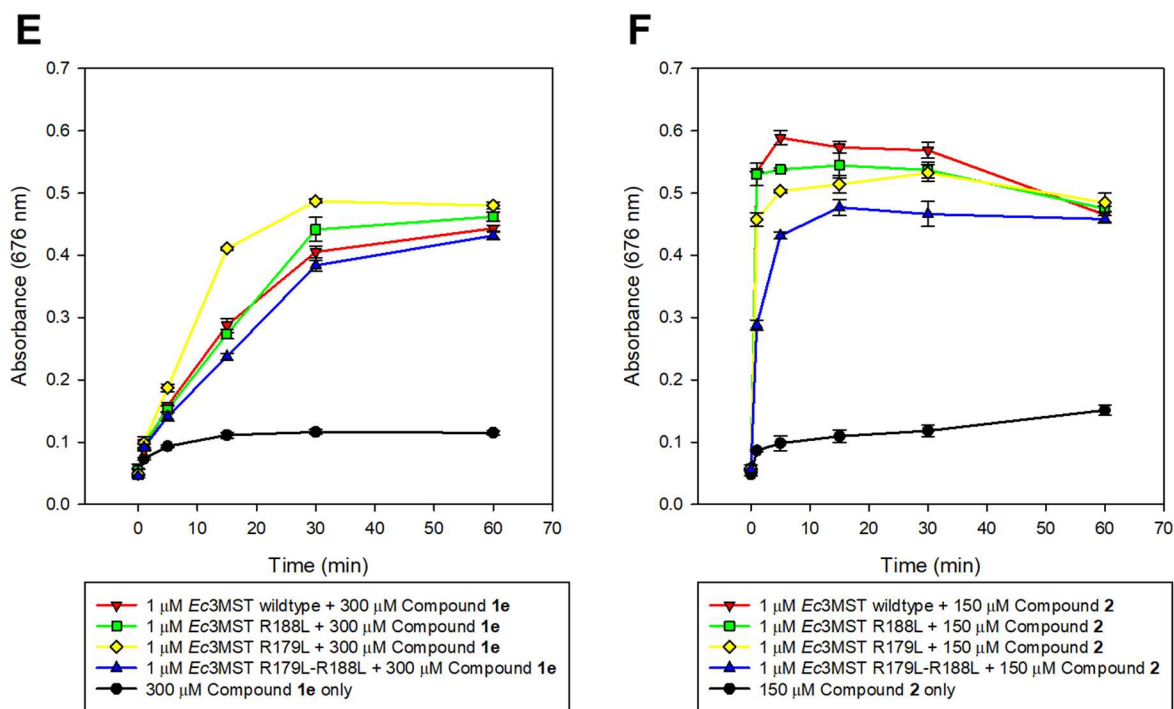


Figure 7: Methylene blue assay to assess the turnover of compounds 1a-e and 2

		Compounds					
		2	1a	1b	1c	1d	1e
At t = 15 min, Absorbance at 676nm in Methylene Blue assay							
Rate	Wild-type	-NA-	$2.04 \pm 0.49 \text{ h}^{-1}$	$1.36 \pm 0.58 \text{ h}^{-1}$	$15.58 \pm 4.00 \text{ h}^{-1}$	$2.70 \pm 0.69 \text{ h}^{-1}$	$3.59 \pm 0.32 \text{ h}^{-1}$
	R188L	-NA-	$2.32 \pm 0.45 \text{ h}^{-1}$	$1.67 \pm 0.36 \text{ h}^{-1}$	$16.68 \pm 5.50 \text{ h}^{-1}$	$3.12 \pm 0.28 \text{ h}^{-1}$	$3.17 \pm 0.79 \text{ h}^{-1}$
	R179L	-NA-	$6.73 \pm 1.6 \text{ h}^{-1}$	1.95 ± 0.21	$14.40 \pm 3.11 \text{ h}^{-1}$	$3.78 \pm 0.53 \text{ h}^{-1}$	$5.79 \pm 1.06 \text{ h}^{-1}$
	R179L/R188L	$49.42 \pm 6.41 \text{ h}^{-1}$	$4.38 \pm 1.02 \text{ h}^{-1}$	$1.46 \pm 0.30 \text{ h}^{-1}$	$11.52 \pm 3.21 \text{ h}^{-1}$	$2.16 \pm 0.33 \text{ h}^{-1}$	$2.72 \pm 0.61 \text{ h}^{-1}$

Table 2: The absorbance recorded in the Methylene Blue assay at t = 15 minutes is plotted for all enzymes and the substrates. The rates were obtained by fitting the curves in Figure 7 with the pseudo-first order rate equation

Since the graphs have almost reached saturation at 15 minutes, the bar graphs for the absorbance values at 15 minutes are plotted in **Table 2** for easier visualization of the data from the Methylene Blue assay.

From the assay, it was observed that wild-type, R179L, R188L, R179L/R188L *Ec3MST* can turn over all the substrates **1a-e** and **2**. The rate of turnover (shown in **Table 2**) was calculated by fitting the activity plot to the pseudo-first order rate equation $y = y_0 + a(1 - e^{-kx})$, where k is the rate constant of the reaction. The fitting of the data was done to the pseudo-first order reaction, and not a second-order reaction because the concentration of the substrate at any given point of time of the reaction is much higher than that of the enzyme. The reaction plot of wild-type, R179L, and R188L *Ec3MST* enzymes with compound **2** could not be fitted to the pseudo-first order reaction since saturation was reached in a very short time.

From **Table 2**, it is evident that among the unnatural substrates **1a-e**, the rate of turnover of compound **1c** by all the *Ec3MST* enzymes is the highest. And the rate of turnover of the compound **1b** by all the *Ec3MST* enzymes is the slowest, and saturation was not reached even after 1 hour.

R179L/R188L Ec3MST has better activity with 1a as compared to wild-type Ec3MST but poorer activity with the natural substrate 3-mercaptopyruvate:

The thiol of compound **1a** gets de-protected in the presence of DTT forming compound **3**. On comparing the structure of **3** and 3-mercaptopyruvate (**Figure 4 (B)**), **3** has a phenyl ring in the place of the carboxyl group of 3-mercaptopyruvate. Thus, in the reaction of **1a** with wild-type *Ec3MST*, the electrostatic interaction between the residues Arg 179 and Arg 188 would only be limited to the carbonyl group adjacent to the phenyl ring in **1a**.

The introduction of leucine residues in place of arginine would create a hydrophobic environment, which may assist the non-polar phenyl ring to be stabilized better in the active-site of R179L/R188L *Ec3MST*. Moreover, the chain length of the leucine residues is shorter as compared to the arginine residues. This results in the introduction of a “pocket” in the active-site, which might contribute to the better stabilization of the phenyl

group of **1a**. The combination of these effects might be responsible for improving the activity of **1a** with R179L/R188L *Ec3MST* (**Figure 7 (A)**).

On the other hand, due to the lack of positively charged arginine residues (Arg 179 and Arg 188) in the R179L/R188L *Ec3MST*'s active-site, 3-mercaptopyruvate might not be able to bind to its active-site as strongly as in the wild-type *Ec3MST*. This is demonstrated by a clear decrease in the activity of R179L/R188L mutant with compound **2** (**Figure 7 (F)**).

The activity of compound 1c is similar with all the Ec3MST enzymes:

In unpublished data from our lab, it has been seen that compound **1c** has better activity than 3-mercaptopyruvate in the case of wild-type *Ec3MST*. From **Figure 7 (C)** and **Table 2**, we can see that the activity and the rate of turnover of all the enzymes with **1c** are almost similar, and **1c** shows higher activity compared to the other unnatural substrates (**1a-e**). This might be because of the electron-withdrawing nature of the *para*-nitrophenol group which decreases the electron density on the carbon adjacent to the thiol group of de-acetylated **1c**, making the sulfur is highly prone to a nucleophilic attack. Hence, the rate of reaction is fast, as seen in **Table 2**, and it almost reaches saturation at 15 minutes. Even in the absence of an enzyme, the amount of H₂S produced by **1c** is comparatively higher than the other phenyl-substituted substrates (**Figure 7 (C)**).

Changing the phenyl group on compound 1a to a naphthyl group does not increase the rate of reaction:

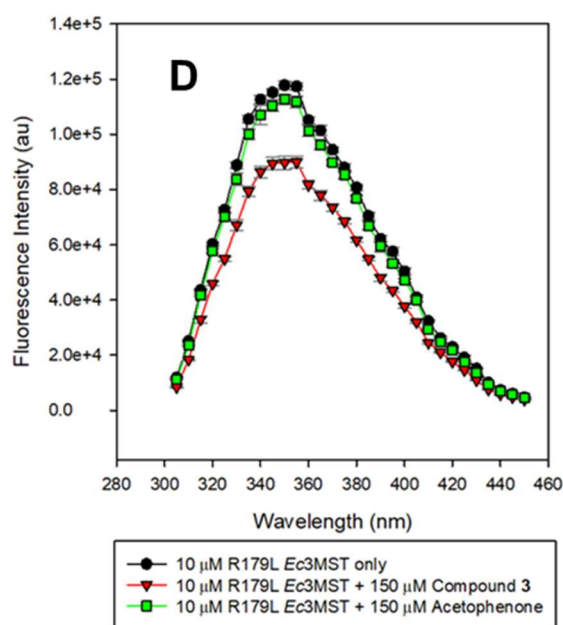
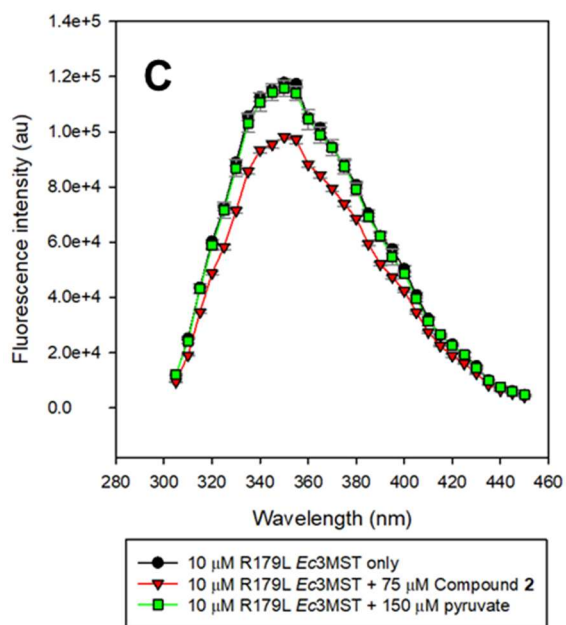
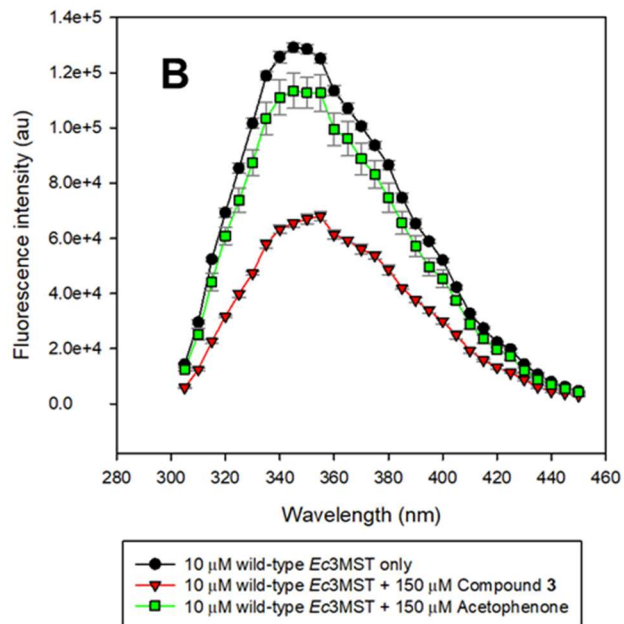
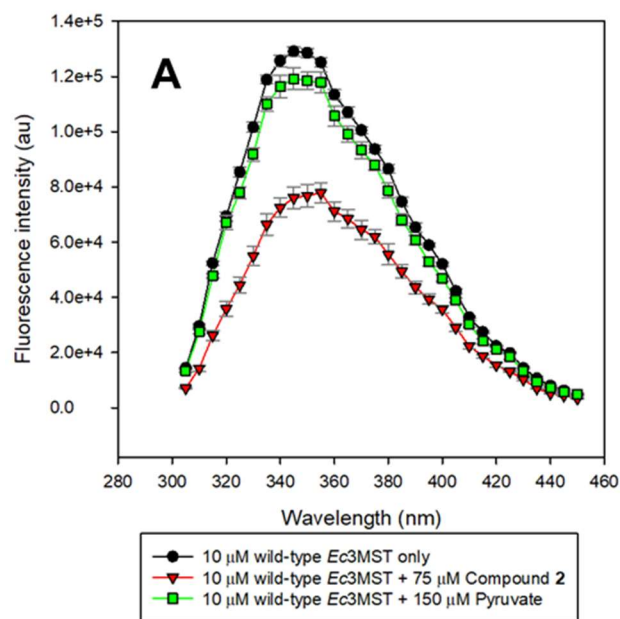
As compound **1a** showed an increase in activity as the hydrophobicity of the active-site increased (R179L/R188L *Ec3MST* has better activity with **1a** as compared to wild-type *Ec3MST*), we expected to see a similar trend with compounds **1d** and **1e**, as they differ from compound **1a** very slightly. **1a** has a benzene ring, whereas compounds **1d** and **1e** have a naphthyl ring. From **Figure 7 (D)** and **(E)** and **Table 2**, we can see that rate of reaction is almost similar across all the *Ec3MST* enzymes.

An explanation for this observation might be the bigger size of the naphthyl ring – which may not be easily accommodated in the active-site as compared to the phenyl ring of compound **3** (de-protected compound **1a**). The larger size may lead to steric clashes, which might result in poor stabilization of the substrate in the active-site.

Change in the intrinsic fluorescence of the enzyme during substrate binding can tell us how well the substrate can bind:

The *Ec3MST* enzyme has eight tryptophan residues overall in its structure with one tryptophan residue (Trp 204) present in the active-site. Tryptophan residues are known to be fluorescent and will show a change in their fluorescence if a substrate binds in the active-site pocket and the conformation of the active-site is changed.

The ratio (F/F_0) of fluorescence intensity of the enzymes co-incubated with the substrate (F) and the fluorescence of the native enzyme (F_0) would tell us the relative amount of decrease of fluorescence. Any changes in the local environment of the tryptophan residue would change its fluorescence. This change might be due to any structural or conformational changes in the protein due to a ligand-binding event. For 3MST, the fluorescence quenching can be due to two reasons. A change in the local environment of the tryptophan due to ligand binding, or due to the conformation change of the protein due to the persulfuration of the active-site cysteine residue after the substrate has been turned over. The change in the intrinsic fluorescence was measured for wild-type, R188L, R179L, and R179L/R188L *Ec3MST* enzymes after being co-incubated with compounds **2** and **3** (**3** is the de-protected compound **1a**).



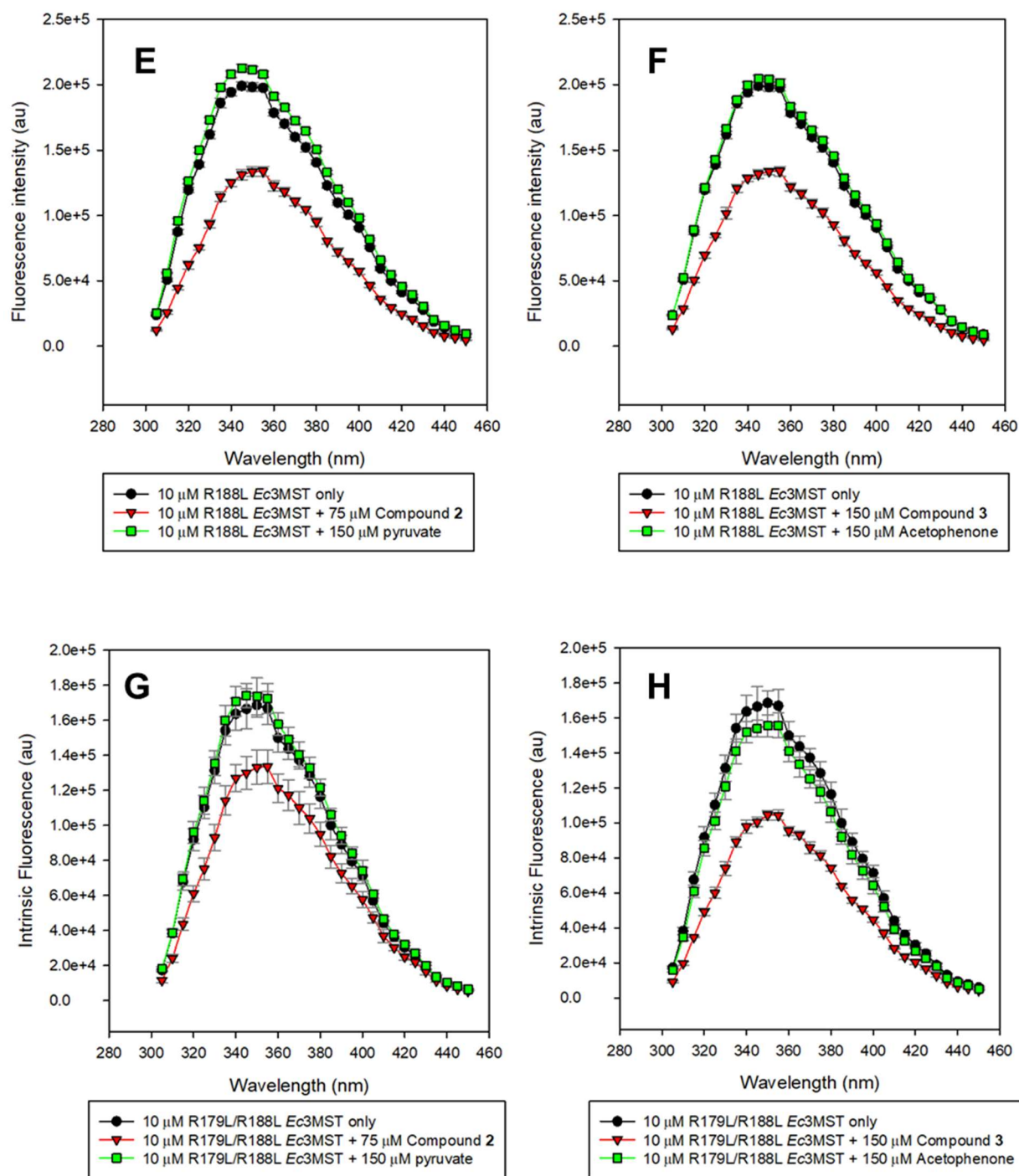


Figure 8: Intrinsic fluorescence change of the enzymes wild-type Ec3MST (A, B), R179L Ec3MST (C, D), R188L Ec3MST (E, F) and R179L/R188L Ec3MST (G, H) when co-incubated with compounds 2, 3, Pyruvate and Acetophenone

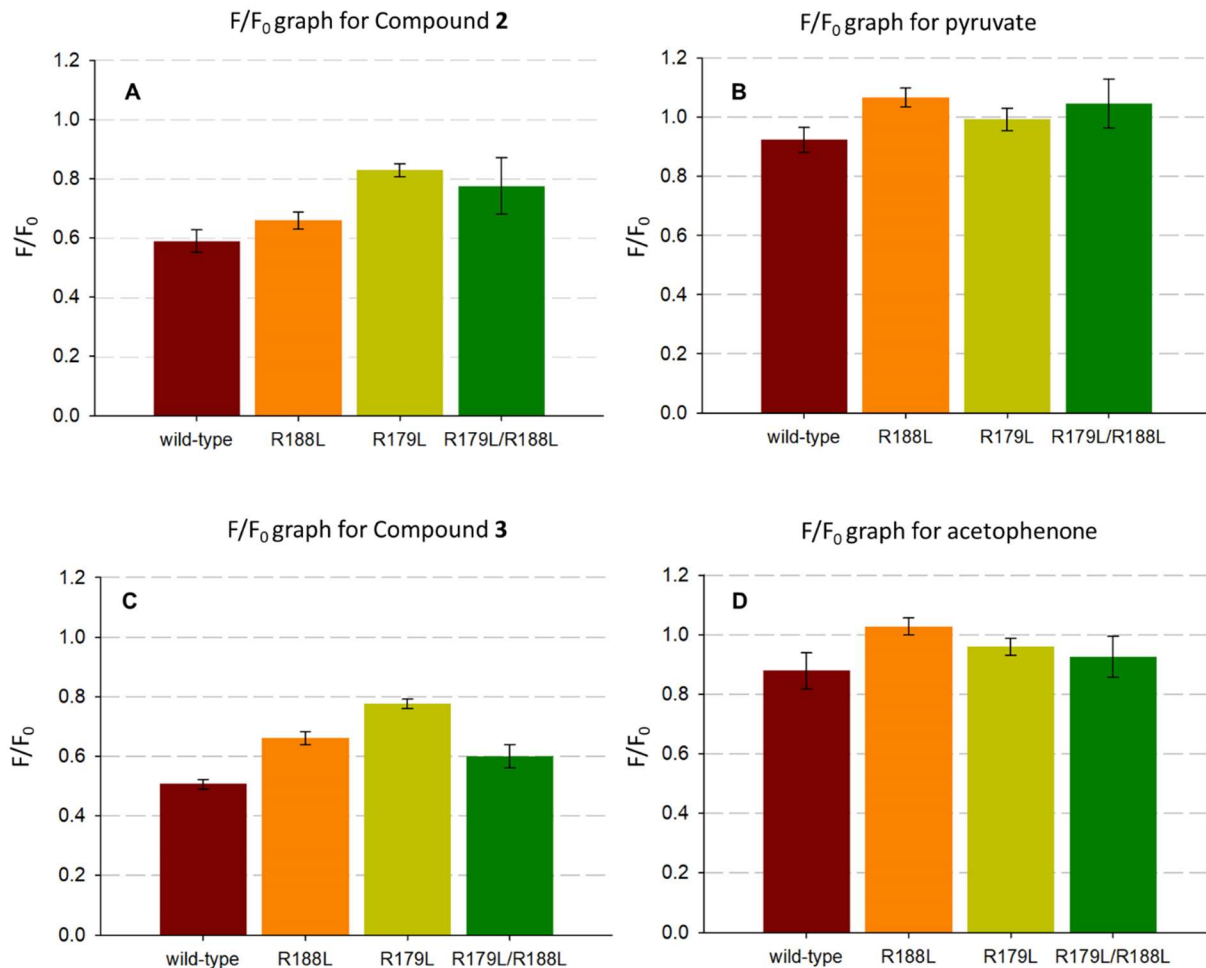


Figure 9: The ratio of fluorescence of the enzyme after co-incubation with the compounds (F) and the fluorescence of the native enzyme (F_0) shows the relative decrease in fluorescence. This figure shows the F/F_0 graphs of all the compounds **2**, **3**, pyruvate and acetophenone with the Ec3MST enzymes

The products of the reaction of Ec3MST with 3-mercaptopyruvate and compound 3 have a poor binding with the enzymes:

The products of the enzymatic reaction with the substrates 3-mercaptopyruvate (formed by the dissociation of compound **2** in presence of HEPES-NaOH pH 7.4 buffer), and compound **3** are pyruvate and acetophenone respectively. When these compounds are co-incubated with the enzymes wild-type, R179L, R188L, and R179L/R188L Ec3MST,

the decrease in the intrinsic fluorescence are very less as compared to the substrates (as seen in **Figure 9**).

This might be because the native enzyme conformation does not allow the binding of the products in the active-site, and only allows the binding of the substrate. Another interpretation of this result is that even though the product molecules bind, the residence time in the enzyme active-site is very small. If the products were to bind in the active-site for a long period of time, it would prevent the entry of incoming substrate molecules, hence resulting in a very poor rate of turnover of the enzyme.

Modeling of Ec3MST:

Sequence alignment of the Ec3MST and h3MST:

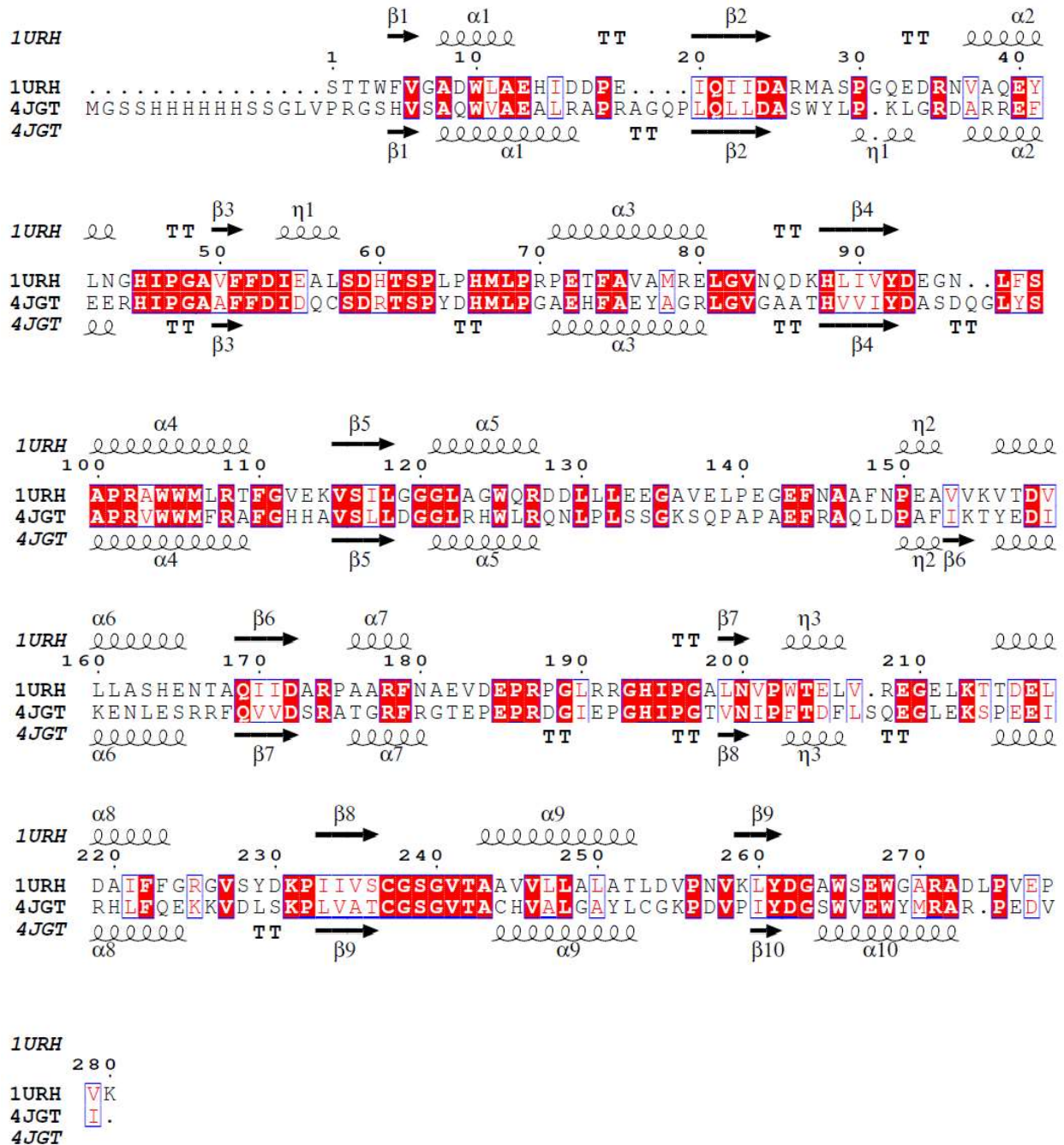


Figure 10: Sequence alignment of Ec3MST (PDB ID: 1URH) and h3MST (PDB ID: 4JGT) showing their structural similarity.

In **Figure 10**, the sequences of *Ec3MST* and h3MST are aligned, along with their respective secondary structure information as obtained from the reported structures in the PDB database (*Ec3MST* PDB ID: **1URH** and h3MST PDB ID: **4JGT**). Their secondary structure information is present in the alignment, where α represents α -helix, β represents β -sheet and η represents the loop regions.

Modeling of *Ec3MST* from h3MST structure (PDB ID: 4JGT):

Although the crystal structure of *Ec3MST* is available (PDB ID: 1URH), docking of molecules in its active-site did not give the correct orientation of the molecules required for the enzymatic reaction. This is because the *Ec3MST* was not co-crystallized with any ligands that can bind to the active-site, hence the active-site conformation available was unsuitable for molecular docking studies. The reported structure of the homolog of *Ec3MST*, human 3MST (h3MST), was co-crystallized with 3-mercaptopyruvate, the natural substrate for 3MSTs. Human 3MST and *Ec3MST* have a sequence identity of 40.5%, but they have very high similarity in their secondary structures (TM-score = 0.8930)⁽²⁵⁾. Also, the active-site residues are very well conserved in these two enzymes. Hence, the modeling of *Ec3MST* based on the scaffold of the reported protein structure of h3MST (PDB ID: 4JGT) would give us a good-confidence model.

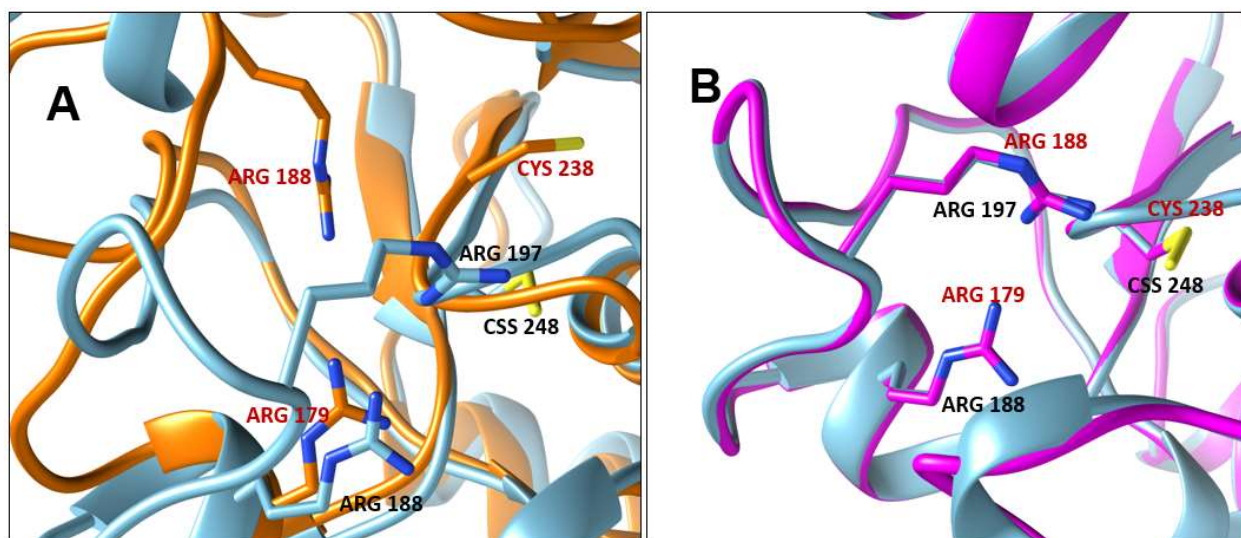


Figure 11: (A) The overlapping active-site residues of the reported h3MST (cyan) and *E. coli* 3MST (orange) protein structures. (B) Modeled structure of *Ec3MST* (magenta) with the scaffold of h3MST (cyan; PDB ID: 4JGT).

In **Figure 11 (A)**, we can see that the Arg 188 residue present on the loop is far from the active-site of the enzyme in the reported crystal structure of *Ec3MST* (orange in **Figure 11 (A)**, PDB ID: 1URH). This is due to the absence of any ligands in the active-site, which allowed any random conformation of the loop. But in case of h3MST protein structure (cyan in **Figure 11 (A, B)**), which has a pyruvate molecule bound in its active-site, has the arginine residue (Arg 197) in the active-site. Hence, after modeling the *Ec3MST* structure based on the template of the h3MST protein structure (PDB ID: 4JGT), we obtain a structure of *Ec3MST* that has both the arginine residue close to the active-site, and can be used for further docking studies.

Docking of substrates in the active-site of modeled wild-type *Ec3MST*:

The orientation of the carboxyl group and the carbonyl groups is similar to the orientation of the docked pyruvate in h3MST. Moreover, the distance between the Cys 238 and the thiol group of 3-mercaptopyruvate is close enough for the reaction to be feasible (**Figure 12**). As reported by a study⁽¹⁶⁾, the electrostatic interaction of the arginine residues and the carbonyl and the carboxyl group of 3-mercaptopyruvate are majorly responsible for binding the substrate in the active-site.

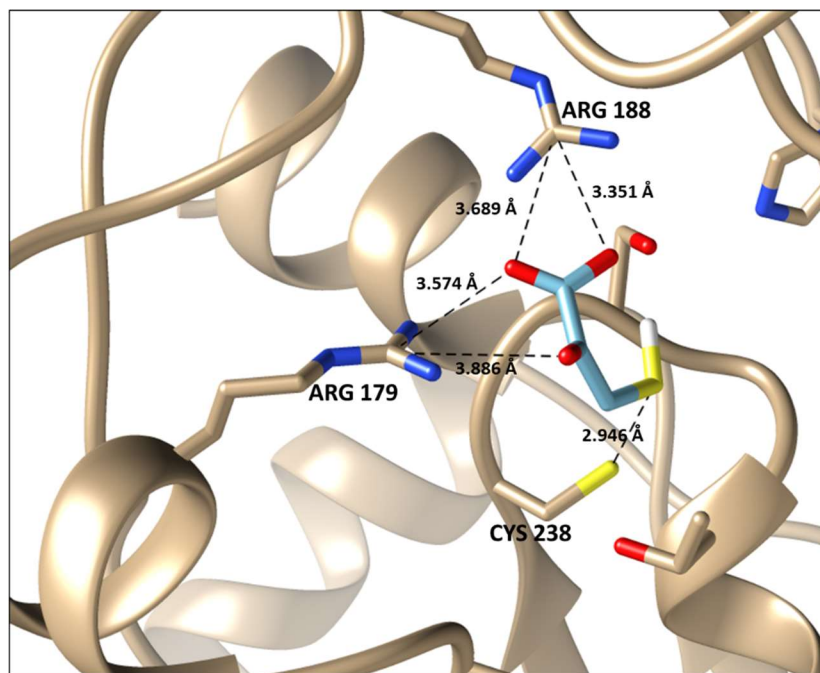


Figure 12: The docked structure of 3-mercaptopyruvate in the active-site of modeled *Ec3MST*

We move on to the docking of the unnatural substrates in order to visualize their interactions with the residues in the active-site. This would help us gain more insights into the reaction mechanism of the unnatural substrates.

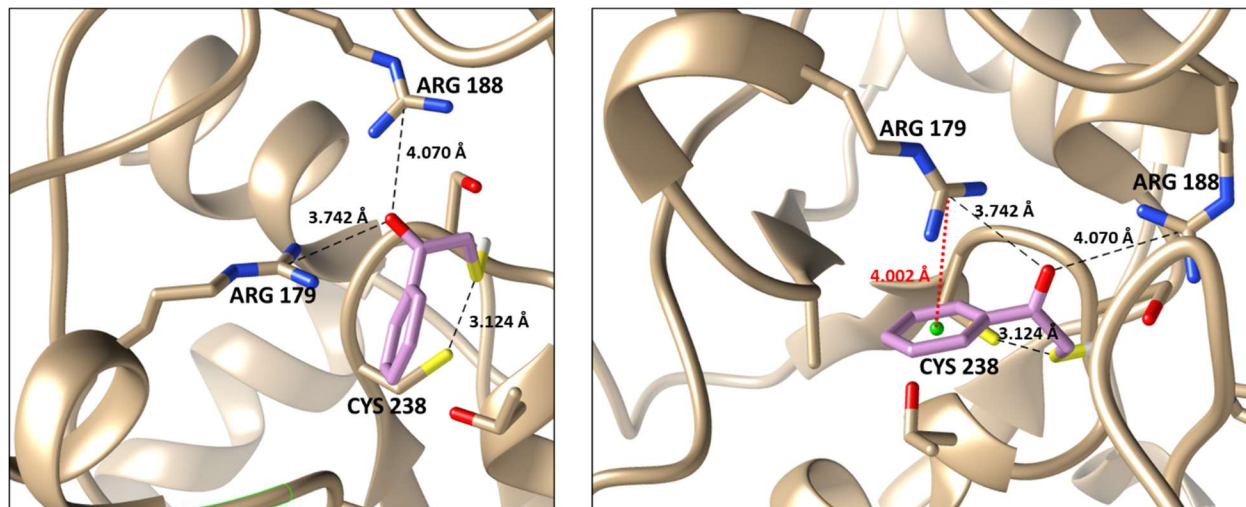


Figure 13: The docked structure of compound **3** in the active-site of modeled Ec3MST. The π -cation interaction of the Arg 179 with the benzene ring is shown by the red-dotted line

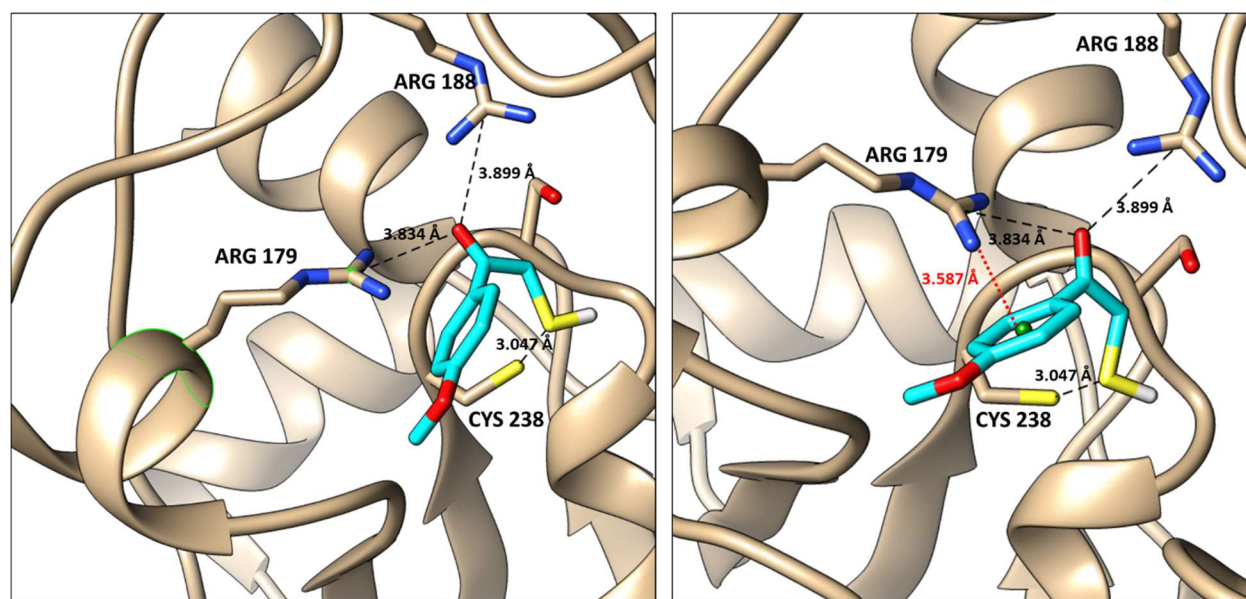


Figure 14: The docked structure of the de-protected compound **1b** in the active-site of Ec3MST. The π -cation interaction of the Arg 179 with the benzene ring is shown by the red-dotted line.

The docked structures of compound **3** and de-protected **1b** reveals interesting insights on the interactions which the unnatural substrates have with the enzyme. Firstly, the binding mode of the molecules is unchanged, where the two arginine residues are still responsible for electrostatically binding the substrate in place (**Figures 13** and **14**). But an additional interaction is revealed that further stabilizes the unnatural substrates in place – a π -cation interaction with the positively charged ARG 179 and the benzene ring of the substrate (shown by a red dotted-line in **Figures 13** and **14**). In literature⁽²⁷⁾, π -cation interactions have been shown to contribute significantly to the binding energy of protein-ligand complexes. Hence, this new interaction might be compensating for the loss of the electrostatic interactions with the carboxyl group of the natural substrate.

Mutating arginine 179 results in better activity with substrate 1a, 1b, 1d, and 1e:

From the bar graphs in **Table 2** and **Figure 7 (A), (B), (D), and (E)**, we can see that the reaction with R179L *Ec3MST* shows the best activity among the wild-type and the mutant *Ec3MST* enzymes. Whereas mutating the Arg 188 does not improve the activity of the enzyme as compared to the R179L mutation.

A possible explanation for this is that mutating Arg 179 disrupts the π -cation interaction (from **Figures 13** and **14**) with the aromatic ring of the substrates, and it opens up the opportunity for the ligand to make a different interaction with some other residues in the active-site, which results in the improved activity of the enzyme. Moreover, due to the shorter chain length of leucine, when the mutation of arginine to leucine is made, it might be allowing the phenyl or naphthyl group to be accommodated better in the active-site due to the proximity of Arg 179 to the aromatic group. The unnatural substrate can then be stabilized better in the active-site, which results in improved activity. More study needs to be done on this to provide any conclusive reason.

Characterizing the activity of h3MST with unnatural substrates

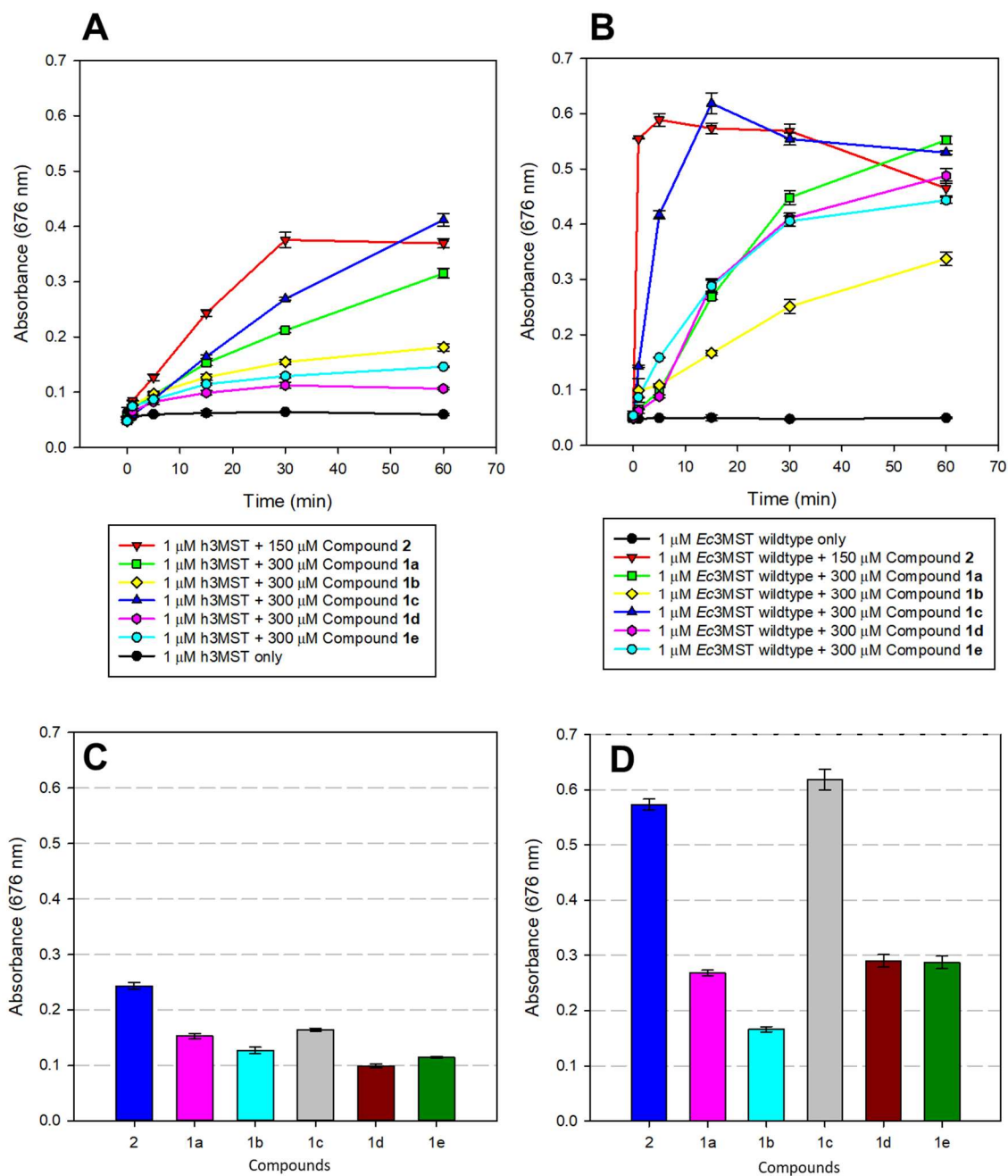


Figure 15: (A-B) Methylene blue assay to assess the turnover of the compounds 1a-e and 2, by h3MST (A) and wild-type Ec3MST (B). (C-D) The absorbance at the 15-minute time point is plotted for h3MST (C) and wild-type Ec3MST (D).

The h3MST has a very similar structure as compared to *Ec3MST*, with a high similarity of residues in the active-site. Hence, it was expected that h3MST and *Ec3MST* would have similar activity with the unnatural substrates. The activity of h3MST was monitored using the Methylene blue assay.

From the data shown above (**Figure 15**), we can clearly see that the h3MST enzyme has very low activity as compared to the *Ec3MST*. Even with the natural substrate, 3-mercaptopyruvate (compound **2** dissociates in the buffer in the presence of DTT to 3-mercaptopyruvate), the rate is slower. In the reaction with wild-type *Ec3MST*, we observe that the maximum activity is reached within 5 minutes with compound **2** whereas saturation is not reached in case of h3MST.

All the substrates show decreased activity in the case of h3MST when compared with *Ec3MST*. Even compound **1c**, which shows the best activity with *Ec3MST* gets turned over at a slower rate with h3MST. The naphthyl substituted compounds **1d** and **1e** show even lesser activity with h3MST. Although the trend in **Figure 15 (C)** and **(D)** are similar, we were not able to explain the decreased activity of h3MST.

An explanation for our observation is that the number of active protein molecules obtained after protein purification might have been low in the case of h3MST. Since there is no way to determine the number of active molecules of proteins, the protein purification was repeated with a different batch of cells, and care was taken to maintain ice-cold conditions during purification to prevent denaturation of the enzyme. The activity of the new batch of h3MST turned out to be similar to what we see in **Figure 15 (A)**.

Another reason for the decreased activity might be that the slight differences between the active-site of h3MST and *Ec3MST* which causes the substrates to be turned over slower in case of h3MST. Hence we take a look at the overlapped active-site of h3MST and *Ec3MST* in **Figure 16** with all the residues within a 5 Å distance within the ligand-binding site.

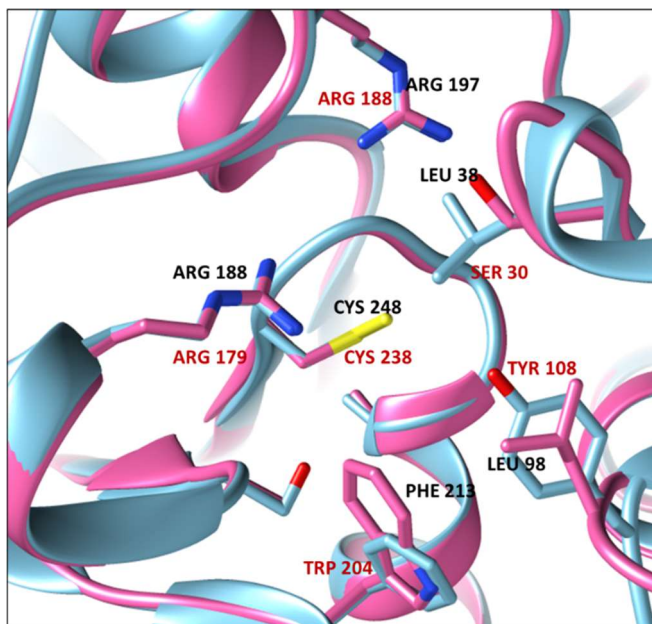


Figure 16: *Overlap of the active-site of Ec3MST and h3MST showing the different residues. Ec3MST structure is shown in pink, and h3MST is shown in cyan. The residues labeled in red are those of Ec3MST, whereas those in black are of h3MST*

Figure 16 shows that the residues that are different in h3MST as compared to *Ec3MST*. Instead of a Ser 30 in *Ec3MST*, there is a Leu 38 in h3MST, which is a hydrophobic residue. Similarly, there is Phe 213 (h3MST) in place of Trp 204 (*Ec3MST*), and Tyr 108 (h3MST) in place of Leu 98. Since all these residues do not contribute to huge changes in polarity and hydrophobicity, any comments on better stabilization of the substrate cannot be made. Thus, no conclusions can be drawn for the low activity just by the active-site information of h3MST.

4. CONCLUSIONS:

This study focuses on the mechanistic investigation of the turnover of unnatural substrates developed in our lab and primarily focuses on the role of the arginine residues responsible for electrostatically holding the substrate in the active-site of *E. coli* 3-mercaptopyruvate sulfurtransferase.

From the methylene blue assay, compound **1a** demonstrated better activity with the double arginine mutant R179L/R188L *Ec3MST*, as compared to the wild-type *Ec3MST* enzyme. Since the highly polar carboxyl group of 3-mercaptopyruvate has been replaced with a non-polar benzene ring in compound **1a**, the binding of the substrate is thought to be better in the mutant protein, which might be responsible for the better activity.

Compounds **1d** and **1e** do not show better activity with the R179L, R188L, and R179L/R188L *Ec3MST* mutant enzymes as compared to **1a**. The increased hydrophobicity of the naphthyl substituted substrates was hypothesized to have better activity due to better stabilization in the active-site of the mutant enzymes. The active-site might not be able to accommodate a larger ring, which might be responsible for the reduced activity as compared to **1a**.

The docking studies revealed interesting insights about the interactions of the substrate **3** and de-protected **1b** with the active-site residues. Since the carboxyl group has been changed to a substituted phenyl group in the unnatural substrates, the π electron density can now form a π -cation interaction with the Arg 179. Although the interaction is not as strong as the electrostatic interactions of 3-mercaptopyruvate and the positively charged arginine residues, this helps the substrate to bind to the active-site better.

The loss of the π -cation interaction in the R179L mutations might be allowing the unnatural substrates **1a**, **1b**, **1d**, and **1e** to interact with some other residues in the active site, which increases the activity of the enzyme as compared to the wild-type *Ec3MST*. The same effect is not observed in the R188L mutants, likely because the π -cation interaction is still present. Moreover, due to the proximity of Arg 179 to the bulky aromatic groups of the unnatural substrate, the R179L mutation might be creating some space in the active-site

that can stabilize the bulky aromatic group better resulting in the increased activity of R179L *Ec*3MST mutant enzymes with the unnatural substrates **1a**, **1b**, **1d**, and **1e**.

5. FUTURE DIRECTIONS:

Moving forward, computational studies aiming to visualize the interactions of the unnatural substrates in the active-site of the mutant proteins would paint a clearer picture regarding the role of Arg 179. This would help answer the questions as to why the R179L mutant has the highest activity with the unnatural substrate amongst the wild-type, R188L, and R179L/R188L double mutants.

Extending the findings of this study, more mutations can be made in the active-site residues and more substrates can be designed in order to aim for obtaining specificity for an unnatural substrate over the natural substrate, 3-mercaptopyruvate. Moreover, since there are no reported inhibitors of *Ec*3MST, gaining more insights into the mechanism of H₂S production would enable us to design inhibitors rationally. This knowledge can then be extended to humans, and drugs that can modulate the endogenous production of H₂S can be designed and used as therapeutics in diseases linked to intracellular H₂S levels.

In a recent study⁽²⁶⁾, a group has demonstrated a targeted and specific release of Nitrogen monoxide (NO), by modifying the β -galactosidase enzyme, and introducing a “hole” in its active-site. The NO-donor molecule designed by the group was also modified by a methyl group, which would perfectly fit the mutant enzyme, but would experience a steric clash with the endogenous β -galactosidase’s active-site. So, when the β -galactosidase mutant enzyme was administered into the target region, followed by intravenous injection of the modified NO-donor, NO was specifically released at the target. We could modify the human 3MST enzyme further to obtain better specificity towards the unnatural substrate and utilize this strategy of targeted delivery of H₂S at a site.

6. REFERENCES:

1. Szabo, C. (2017). A timeline of hydrogen sulfide (H₂S) research: from environmental toxin to biological mediator. *Biochem. Pharmacol.*, S0006–2952(17)30606-8
2. Vigneaud, V., Loring, H. S., and Craft, H. (1934). The oxidation of the sulfur of homocystine, methionine, and S-methylcysteine in the animal body. *J. Biol. Chem.*, 105, 481
3. Binkley, F., and Vigneaud, V. (1942). The formation of cysteine from homocysteine and serine by liver tissue of rats. *J. Biol. Chem.*, 144, 507
4. Warenycia, M. W., Goodwin, L. R., Benishin, C. G., Reiffenstein, R. J., Francom, D. M., et al. (1989). Acute hydrogen sulfide. Demonstration of selective uptake of sulfide by the brainstem by measurement of brain sulfide levels. *Biochem. Pharmacol.*, 38, 973–981
5. Goodwin, L. R., Francom, D., Dieken, F. P., Taylor, J. D., Warenycia, M. W., et al. (1989). Determination of sulfide in brain tissue by gas dialysis/ion chromatography: postmortem studies and two case reports. *J. Anal. Toxicol.*, 13, 105–109
6. Tang, G., Wu, L., Liang, W., and Wang, R. (2005). Direct stimulation of K(ATP) channels by exogenous and endogenous hydrogen sulfide in vascular smooth muscle cells. *Mol. Pharmacol.*, 68, 1757–1764
7. Wang, R. (2012). Physiological implication of hydrogen sulfide: a whiff exploration that blossomed. *Physiol. Rev.*, 92, 791–896
8. Pal, V. K., Bandyopadhyay, P., & Singh, A. (2018). Hydrogen sulfide in physiology and pathogenesis of bacteria and viruses. *IUBMB Life*, 70(5), 393–410
9. Predmore, B. L., Lefer, D. J., and Gojon, G. (2012). Hydrogen sulfide in biochemistry and medicine. *Antioxid. Redox Signal*, 17, 119–140
10. Wang R. (2002). Two's company, three's a crowd: can H₂S be the third endogenous gaseous transmitter? *FASEB J.*, 16, 1792-1798

11. Shatalin, K.; Shatalina, E.; Mironov, A.; Nudler, E. (2011). H₂S: A Universal Defense against Antibiotics in Bacteria. *Science*, (80-) 334 (6058), 986–990
12. Kohanski, M. A., Dwyer, D. J., Hayete, B., Lawrence, C. A., & Collins, J. J. (2007). A Common Mechanism of Cellular Death Induced by Bactericidal Antibiotics. *Cell*, 130(5), 797–810
13. Shukla, P., Khodade, V. S., Sharathchandra, M., Chauhan, P., Mishra, S., Siddaramappa, S., et al. (2017). “On demand” redox buffering by H₂S contributes to antibiotic resistance revealed by a bacteria-specific H₂S donor. *Chem. Sc.*, 8(7), 4967–4972
14. Li, Q. Jr., and Lancaster, J. R. (2013). Chemical foundations of hydrogen sulfide biology. *Nitric Oxide*, 35, 21–34
15. Carballal, S., Trujillo, M., Cuevasanta, E., Bartesaghi, S., Moller, M. N., et al. (2011). Reactivity of hydrogen sulfide with peroxynitrite and other oxidants of biological interest. *Free Radic. Biol. Med.* 50, 196–205
16. Liu, Y., & Imlay, J. A. (2013). Cell death from antibiotics without the involvement of reactive oxygen species. *Science* 339, 1210
17. Yadav, P. K., Yamada, K., Chiku, T., Koutmos, M., & Banerjee, R. (2013). Structure and kinetic analysis of H₂S production by human mercaptopyruvate sulfurtransferase. *J. Biol. Chem.*, 288(27), 20002–20013
18. Lec, J. C., Boutserin, S., Mazon, H., Mulliert, G., Boschi-Muller, S., & Talfournier, F. (2018). Unraveling the Mechanism of Cysteine Persulfide Formation Catalyzed by 3-Mercaptopyruvate Sulfurtransferases. *ACS Cat.*, 8(3), 2049–2059
19. Hanaoka, K., Sasakura, K., Suwanai, Y., Toma-Fukai, S., Shimamoto, K., Takano, Y., et al. (2017). Discovery and mechanistic characterization of selective inhibitors of H₂S -producing Enzyme: 3-Mercaptopyruvate. *Scientific Reports*, 7, 1-7
20. Fukuto, J. M., Ignarro, L. J., Nagy, P., Wink, D. A., Kevil, C. G., Feelisch, M., Akaike, T. (2018). Biological hydropersulfides and related polysulfides – a new concept and perspective in redox biology. *FEBS Letters*, 592(12), 2140–2152

21. Leggett, D. J.; Chen, N. H.; Mahadevappa, D. S. (1981). Flow Injection Method for Sulfide Determination by the Methylene Blue Method. *Anal. Chim. Acta*, 128, 163–168
22. Morris, G. M., Huey, R., Lindstrom, W., Sanner, M. F., Belew, R. K., Goodsell, D. S. and Olson, A. J. (2009). Autodock4 and AutoDockTools4: automated docking with selective receptor flexibility. *J. Comp. Chem.*, 16, 2785-91
23. Roy, A., Kucukural, A., Zhang, Y. (2010). I-TASSER: a unified platform for automated protein structure and function prediction, *Nature Protocols*, 5, 725-738
24. Yang, J., Yan, R., Roy, A., Xu, D., Poisson, J., Zhang, Y. (2015). The I-TASSER Suite: Protein structure and function prediction, *Nature Methods*, 12, 7-8
25. Zhang, Y., Skolnick, J. (2004). Scoring function for automated assessment of protein structure template quality, *Proteins*, 57, 702–710
26. Hou, J., Pan, Y., Zhu, D., Fan, Y., Feng, G., Wei, Y., Wang, H., Qin, K., Zhao, T., Yang, Q., et al. (2019). Targeted delivery of nitric oxide via a 'bump-and-hole'-based enzyme–prodrug pair, *Nat. Chem. Biol*, 15, 151-160
27. Dougherty, D. (2013). The Cation- π Interaction, *Acc Chem Res*, 46(4): 885–893